HUBBLE SPACE TELESCOPE ZERO GYRO SUN POINTING WITH A KALMAN FILTER

Sun H. Hur-Diaz
Emergent Space Technologies, Inc.

Jim Seidel
Lockheed Martin Space Systems

ABSTRACT

An improved zero gyro safemode was designed for the Hubble Space Telescope based on the Multiplicative Extended Kalman Filter using magnetometer and sun sensor measurements. The filter estimates the vehicle angular rate and inertial quaternion enabling control of the sun pointing error even during orbit night to keep the vehicle at sun pointing attitude at all times.

INTRODUCTION

As the gyros on the Hubble Space Telescope (HST) age and become ineffective, a sun pointing safemode with no reliance on gyro measurements becomes important. The current zero gyro sun pointing (ZGSP) safemode has had acceptable performance, but there were instances when the pointing had drifted by more than 100 degrees. A full description of ZGSP is given in Reference 1. Looking forward to the eventual de-orbiting scenario, where a de-orbit module (DM) would rendezvous and dock with the HST, it was found necessary to improve the ZGSP to satisfy the requirements of the DM mission. In the Servicing Mission 3A (SM3A), for instance, the baselined safemode for the space shuttle rendezvous was the Hardware Sun Point (HWSP) mode with the utilization of the backup gyros instead of ZGSP because of large errors observed in ZGSP (ref. 2). Note that during SM3A, a more advanced main computer that is 20 times faster with six times more memory than its predecessor was installed on HST providing much more processing power and allowing for future software enhancements such as the current Kalman filter.

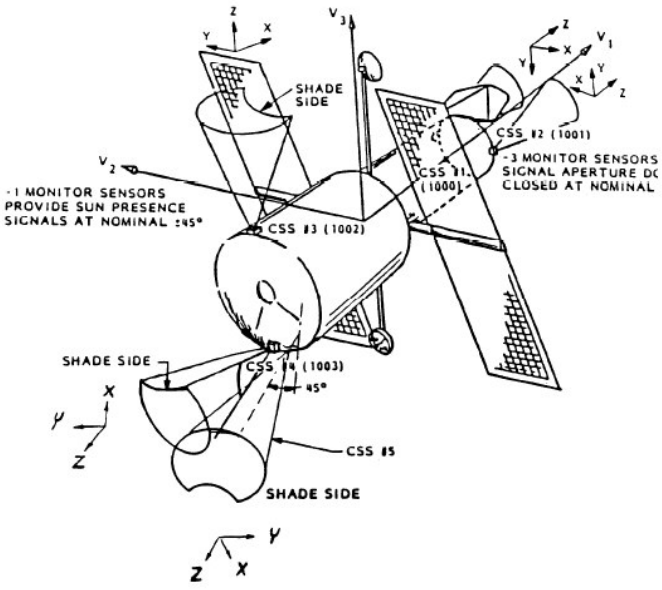

Figure 1. CSS location and orientation

The current ZGSP relies on data from one of five Coarse Sun Sensors (CSS) to achieve and maintain sun pointing during orbit day. The locations of the CSS's and their fields-of-view (FOV) are shown in Figure 1. CSS 1 and 2 are along the V1 axis, CSS 3 is along V3 axis, CSS 4 is along the –V1 axis, and CSS 5 is along the –V1 with a slight cant toward –V3 axis. ZGSP uses CSS data for position and rate information

about the axes perpendicular to the Sun line. It also relies on the 3-axis Magnetic Sensing System's (MSS) magnetic field vector for rate damping about the Sun line. The reaction wheel assembly (RWA) is used for primary attitude control, and the magnetic torquers (MT) are used for momentum management. During orbit night, there is no active sun pointing feedback control, and no commands are sent to the RWA or the MT. To reduce the inevitable drift from the sun pointing attitude, a momentum bias is applied on the RWA for stiffness.

To minimize the drift during orbit night, active feedback control is required. This requires accurate knowledge of the vehicle attitude and rate which is difficult to obtain by simple processing of magnetic field measurements alone. However by utilizing the vehicle dynamics as in a Kalman filter, more accurate estimates of the inertial attitude quaternion as well as the 3-axis angular rates can be obtained.

A high-level block diagram of the improved zero-gyro safemode with the Kalman filter in the loop is shown in Figure 2. Measurements for the Kalman filter are the same as in ZGSP: magnetic field vector from the MSS, which is always available, and the sun vector from an illuminated CSS available during orbit day. The actuators of the safing control system remain the same as well: the RWA for pointing control and the MT for momentum management. With the Kalman filter, attitude and rate estimates are always available, and the vehicle is continuously controlled to sun-pointing attitude even during orbit night.

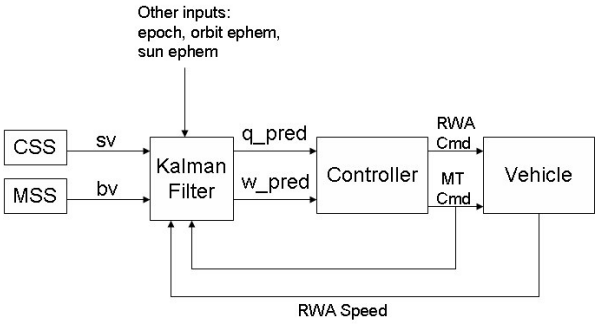

Figure 2. High-level diagram of the zero gyro safemode with Kalman filter in the loop.

KALMAN FILTER DESIGN

The design of a Kalman filter is discussed much in the literature. A good reference is by Gelb (ref. 3). It involves modeling the system and the measurements in terms of the states that are to be estimated and characterizing the expected model uncertainties. The Kalman filter involves two stages: a measurement update and a time update as shown in Figure 3. The system model is used in the time update for predicting states between measurements. The measurement model is used for updating the states with the measurements. The typical nomenclature is that "+" indicates the states after the measurement update, and the "-" indicates the states after the time-update. In the figure, $\vec{x}$ denotes the states, P denotes the covariance matrix of the states, and the subscript k represents the one second measurement sampling intervals.

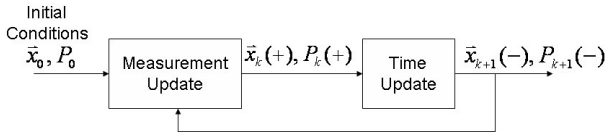

Figure 3. Kalman filter stages

System Model

The system is usually modeled by the time derivative of its states and noise $\vec{w}$ assumed to be Gaussian with zero mean and spectral density Q:

$$\dot{\vec{x}} = \vec{f}(\vec{x},t) + \vec{w}(t), \quad \vec{w}(t) \sim N(0, Q(t)) \tag{1}$$

For the zero gyro sun pointing problem, the desired estimates are the attitude quaternion and the 3-axis attitude rate for feedback into the safemode controller. So at a minimum we need to include them in our

state set. Since operation of the HST in safemode can involve large angles, the basic kinematic and dynamic system equations describing HST attitude are nonlinear. Therefore an extended Kalman filter (EKF) design is required where the equations are linearized about the latest estimate from the measurement update at each sample period:

$$F(\vec{x}_k(+),t) \equiv \left.\frac{\partial f(\vec{x},t)}{\partial \vec{x}}\right|_{\vec{x}=\vec{x}_k(+)} \tag{2}$$

The basic equations for an extended Kalman filter are fully described in Reference 3 and will not be repeated here.

The unity constraint of the quaternion is handled in the manner of the method of Multiplicative Extended Kalman Filter (MEKF) which is described in Reference 4. Essentially, MEKF estimates the 4-dimensional unit quaternion by actually estimating a 3-component attitude error, $\vec{a}$, about a reference unit quaternion, $\vec{q}_{ref}$. So the true quaternion can be represented as $\vec{q} = \vec{q}_e(\vec{a}) \otimes \vec{q}_{ref}$ where $\vec{q}_e$ is the error quaternion approximated by

$$\vec{q}_e \approx \begin{bmatrix} \vec{a}/2 \\ 1 \end{bmatrix} \tag{3}$$

and $\otimes$ represents quaternion multiplication. The time derivative of $\vec{a}$, to first order, can be shown to be (ref. 4):

$$\dot{\vec{a}} = \vec{\omega} - \vec{\omega}_{ref} - \tfrac{1}{2}(\vec{\omega} + \vec{\omega}_{ref}) \times \vec{a} \tag{4}$$

where $\vec{\omega}$ is the total angular rate, and $\vec{\omega}_{ref}$ is the angular rate of the reference attitude. The reference unit quaternion is updated after the measurement update through a reset procedure which is described later in this paper.

Measurement Model

The measurement model consists of a nonlinear function of the predicted states at the time of the measurement plus noise $\vec{v}$ assumed to be Gaussian with zero mean and covariance *R*:

$$\vec{z}_k = \vec{y}(\vec{x}_k(-),t_k) + \vec{v}_k, \quad \vec{v}_k \sim N(0,R_k) \tag{5}$$

As in the system model, the measurement equations are linearized, but about the predicted states:

$$Y_k \equiv \left.\frac{\partial \vec{y}(\vec{x},t_k)}{\partial \vec{x}}\right|_{\vec{x}=\vec{x}_k(-)} \tag{6}$$

Measurement Equations

The measurements considered in the current design consist of the unit magnetic field vector and the unit sun vector both in the vehicle frame as derived from the MSS and the illuminated CSS, respectively. Note that the linear FOV (roughly 45 deg) of the five CSS's do not overlap; therefore a valid sun-vector measurement will not be available at certain attitudes even during orbit day. In general, the vector measurements are a function of the inertial quaternion. The measurement equation for the magnetic field vector is:

$$\hat{b}_V = A(\vec{q})\hat{b}_I + \vec{v}_{MSS} \tag{7}$$

where

$$\begin{aligned} \hat{b}_I &= \text{unit mag field vector in inertial frame computed from model, epoch, and orbit} \\ A(\vec{q}) &= \text{direction cosine matrix (DCM) from inertial to vehicle frame} \\ \hat{b}_V &= \text{unit mag field vector in vehicle frame} \end{aligned} \tag{8}$$

The measurement equation for the sun vector is similar except that an extra rotation due to measurement biases is included:

$$\hat{s}_V = A(\vec{q}_b)A(\vec{q})\hat{s}_I + \vec{v}_{CSS} \tag{9}$$

where

$$\begin{aligned} \hat{s}_I &= \text{unit sun vector in inertial frame obtained from sun ephemeris} \\ A(\vec{q}_b) &= \text{DCM corresponding to sensor biases in vehicle frame} \\ \hat{s}_V &= \text{unit sun vector in vehicle frame} \end{aligned} \tag{10}$$

The measurement bias is to account for low-frequency errors due to uncalibrated albedo. Note that a CSS measurement actually consists of delta angles of the sun from the boresight which are converted to a unit vector in the CSS frame and then transformed into the vehicle frame. Only when the sun is in the linear range of the CSS is the measurement used in the Kalman filter. The MSS measurement, on the other hand, is available and used at all times.

The albedo errors on the CSS can be included in the measurement model as a function of the attitude relative to Earth and the local solar time of the vehicle. However, the approach taken in this design is to model it as a first-order Gauss Markov process and include it as states to be estimated:

$$\dot{\vec{a}}_b = -\vec{a}_b / \tau_b + \vec{w}_{ab} \tag{11}$$

where τ_b is the correlation time constant of the measurement bias state, and $\vec{w}_{ab}$ is the noise representing how well the model approximates the low-frequency errors. The correlation time constant can be selected to be the time constant of the autocorrelation function of the true measurement error. For CSS, a value of 400 seconds provides a good fit of the model to the simulated errors.

System Equations

With the measurement bias state included, the MEKF consists of the following nine states:

$$\vec{x} = \begin{bmatrix} \vec{a} \\ \vec{\omega} \\ \vec{a}_b \end{bmatrix} \tag{12}$$

whose time derivative is given by

$$\vec{f} \equiv \begin{bmatrix} \vec{f}_a \\ \vec{f}_\omega \\ \vec{f}_{ab} \end{bmatrix} = \begin{bmatrix} \vec{\omega} - \vec{\omega}_{ref} - \frac{1}{2}(\vec{\omega} + \vec{\omega}_{ref}) \times \vec{a} \\ I^{-1}\left(- S(\vec{\omega}) I\vec{\omega} + S(\vec{h})\vec{\omega} + \vec{G}(\vec{a}) - \dot{\vec{h}} + \vec{T}_C \right) \\ -\vec{a}_b / \tau_b \end{bmatrix} \tag{13}$$

where I is the inertia matrix, $\vec{h}$ is the RWA angular momentum, $\vec{T}_C$ is the commanded torque to the magnetic torquers, and $\vec{G}$ is the gravity gradient term given by

$$\begin{aligned} \vec{G}(\vec{a}) &= \frac{3\mu}{R_o^3} S(\hat{r}_V(\vec{a})) I \hat{r}_V(\vec{a}) \\ \hat{r}_V(\vec{a}) &= A(\vec{q}_e(\vec{a}))A(\vec{q}_{ref})\hat{r}_I \\ &\approx \left[I_{3\times 3} - S(\vec{a})\right] A(\vec{q}_{ref})\hat{r}_I \quad \text{(to first - order in } \vec{a}) \end{aligned} \tag{14}$$

where R_o is the magnitude of the orbit radius, $\hat{r}_I$ is the unit radius vector in inertial frame, and μ is the gravitational constant. The symbol $S(\,)$ represents the cross-product matrix of a vector:

$$S(\vec{v}) \equiv \begin{bmatrix} 0 & -v_3 & v_2 \\ v_3 & 0 & -v_1 \\ -v_2 & v_1 & 0 \end{bmatrix} \tag{15}$$

In addition to the nine states, the reference quaternion is propagated by the following equation:

$$\dot{\vec{q}}_{ref} = \frac{1}{2} \begin{bmatrix} \vec{\omega}_{ref} \\ 0 \end{bmatrix} \otimes \vec{q}_{ref} \,. \tag{16}$$

Reset Operation

In the MEKF, the following reset operation is performed after a measurement update:

$$\begin{aligned} &1.\quad \vec{q}_{ref}(+) = \vec{q}_e(\vec{a}_k(+)) \otimes \vec{q}_{ref}(-) \\ &2.\quad \vec{q}_{ref}(+) = \vec{q}_{ref}(+) / \left| \vec{q}_{ref}(+) \right| \\ &3.\quad \vec{\omega}_{ref}(+) = \vec{\omega}_k(+) \\ &4.\quad \vec{a}_k(+) = 0 \end{aligned} \tag{17}$$

Note that the reset operation is essentially a measurement update of the reference quaternion and the reference angular velocity. The high-level MEKF process is summarized in Figure 4.

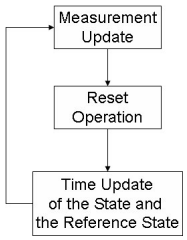

Figure 4. MEKF Process

Selection of Measurement Noise Covariance

The noise covariance matrix of the measurement model is selected based on expected measurement errors. For the magnetic field vector model, error sources include random, quantization, and low frequency errors such as magnetic field modeling error, uncompensated alignment error, vehicle induced magnetic field, and orbit ephemeris error. The total error is estimated to be less than 2.5 deg. Converting this to radians, the measurement noise covariance matrix is

$$R_{MSS} = \left(2.5\frac{\pi}{180}\right)^2 I_{3x3} \approx (0.002) I_{3x3} \quad \text{rad}^2 \tag{18}$$

where I_{3x3} is a 3-by-3 identity matrix. The sun vector measurement model has similar error sources except that there are larger uncompensated errors like albedo. Assuming that a significant portion of this error is accounted for by the measurement bias state, the total remaining error is estimated to be less than 2 deg:

$$R_{CSS} = \left(2\frac{\pi}{180}\right)^2 I_{3x3} \approx (0.001) I_{3x3} \quad \text{rad}^2 \tag{19}$$

Selection of System Noise Parameter

Unlike the measurement model which is based on discrete sampled measurements, the system model is continuous. Therefore, the system noise is characterized by its spectral density function then later converted to covariance matrix to be used with the state error covariance time-update equations. In general, the selection of Q or the equivalent covariance matrix Q_d has to be done carefully in relation to measurement noise and is usually specified based on nonlinear time-domain simulations.

We assume that each state's system noise is independent of the others, and the system noise covariance is given in the following form:

$$Q_d = \begin{bmatrix} Q_a \times I_{3\times3} & O_{3\times3} & O_{3\times3} \\ O_{3\times3} & Q_\omega \times I_{3\times3} & O_{3\times3} \\ O_{3\times3} & O_{3\times3} & Q_{ab} \times I_{3\times3} \end{bmatrix} \tag{20}$$

where O_{3x3} is a 3-by-3 matrix of zeros. From simulations, the following values are found to give satisfactory performance:

$$\begin{aligned} Q_a &= 0 \text{ rad}^2/\text{sec}^2 \\ Q_\omega &= 1\times10^{-10} \text{ rad}^2/\text{sec}^4 \\ Q_{ab} &= 1\times10^{-6} \text{ rad}^2/\text{sec}^2 \end{aligned} \tag{21}$$

In practice, a small nonzero value of Q_a would make the filter more robust.

INITIALIZATION

By proper initialization, the probability of divergence due to large initial errors is reduced. It also leads to faster convergence enabling earlier control activation and faster sun capture after switching to zero-gyro Kalman filter (ZGKF) safemode. On the other hand, if the filter has had a long time to converge and is continuously running in the background outside of the safemode, initialization is not as critical.

Continuous background process, however, would be a waste of onboard computer resources unless the filtered estimates are used for other purposes like monitoring.

Initialization involves assignment of initial values for the states, error covariance matrices, and the reference states. For HST whose rates are usually small on the order of 0.1 deg/sec, an initial rate of zero with a conservative 5 deg/sec uncertainty provides adequate transient performance. The attitude and bias states are also initialized to zero with an uncertainty of about 30 deg. The initial reference quaternion has a bigger impact on the convergence. When both the magnetic field vector and sun vector measurements are available, the initial reference quaternion can be estimated from any two-vector attitude determination algorithm, e.g. the *q*-method described in Wertz (ref. 5). When only the magnetic field vector is available, the same algorithm can be employed using the magnetic field rate as the second vector measurement approximated from back-differencing the filtered MSS measurements. This assumes that the vehicle rate is small compared to the rate of change of the magnetic field vector which averages about 0.08 deg/sec for the HST orbit. Since the vehicle rate can be higher, the initial attitude estimate about the magnetic field vector is expected to be poor.

SUN POINT CONTROLLER

In addition to ZGSP, HST has Software Sun Point (SWSP) and Hardware Sun Point (HWSP) safemodes. SWSP is used when at least three gyros are available. HWSP is used when a failure has been detected that necessitates the use of the backup computer. Both modes have similar control algorithms with RWA for pointing control and MT for momentum management. When there are less than three gyros available, HWSP is an optional safemode with the backup gyros instead of ZGSP. However, because of the limited life of the backup gyros, it is not desirable to go to HWSP unless deemed necessary as in SM3A.

With ZGKF, the full 3-axis rate and attitude information are available than can be fed into the existing SWSP controller as if gyro measurements are available. Furthermore, position feedback can be performed even during orbit night with the sun-pointing error derived from the inertial quaternion estimate. Since the rate estimates from the ZGKF have larger errors than the gyro measurements, the original controller gains will have to be adjusted. To preserve the high bandwith for initial capture, conditional gains are utilized where high gains are used when the pointing error is above a certain threshold, and the low gains are used when the pointing error is below the threshold. A simplified diagram of the controller is shown in Figure 5.

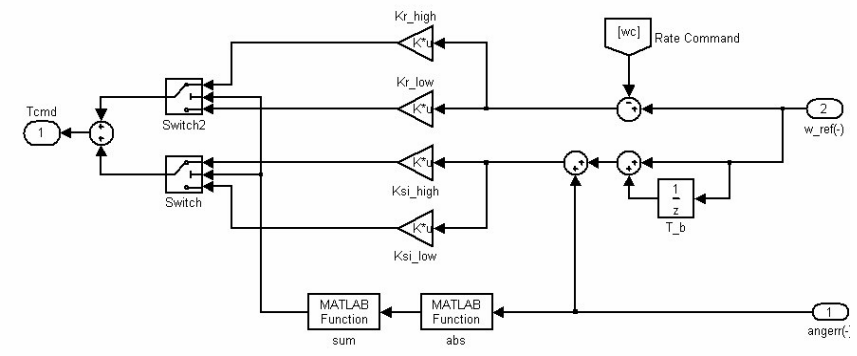

Figure 5. Sun Point Control Law

The input “angerr” is the pointing error relative to the desired sun point control axis derived from the inertial quaternion.

SIMULATION

A sample simulation comparing the performance of ZGSP and ZGKF with inertias corresponding to HST with the de-orbit module attached was performed. The sun point control axis was V3. The initial pointing error was 150 degrees, and initial rate was [.071 .076 0] deg/sec. The sun angle and rate histories are shown in Figures 6 and 7, respectively. The square waves shown correspond to orbit daytimes. The first plot in each figure corresponds to the ZGSP response simulated in high-fidelity safing simulation written in Advanced Continuous Simulation Language (ACSL) and FORTRAN. The second plot corresponds to ZGKF response simulated in Matlab/Simulink. The third plot is a close-up of the ZGKF response. The controllers are slightly different between the two simulations. The ZGSP used the SWSP control law with high gains. The ZGKF used the HWSP control law with low gains and even lower gains after sun capture.

Figure 6 shows that ZGSP initially captures the sun faster but with a higher overshoot than ZGKF because of the higher gains. However, orbit night excursions are quite high such that when the vehicle enters orbit day again, the sun has to be recaptured. In some instances, the recapture takes almost the entire duration of the orbit day. ZGSP response, on the other hand, is more consistent, and the sun angle error remains below 5 degrees after the initial capture.

Figure 7 shows the vehicle angular rate history. In ZGSP, the rates get high at times when the sun has to be recaptured upon entering orbit day. In ZGKF, the pointing error remains small enough that high rates are not seen, and the rates stay below 0.01 deg/sec after the initial capture.

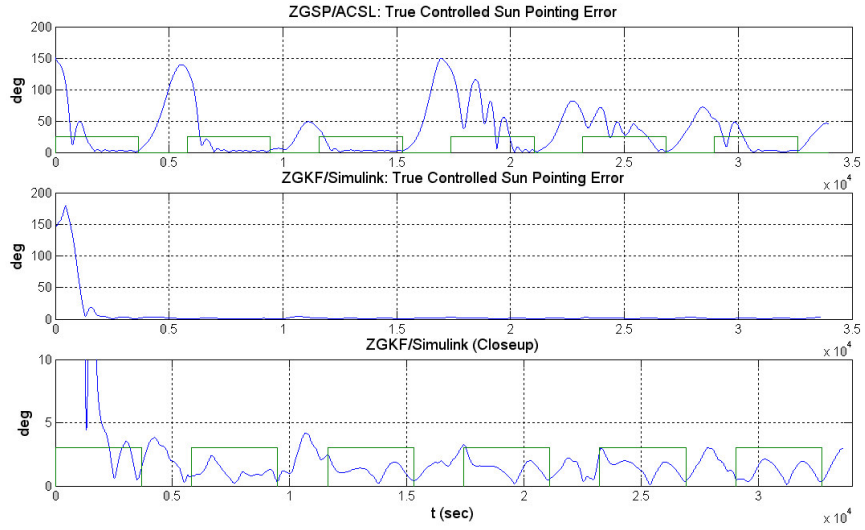

Figure 6. Comparison of sun angle history for ZGSP and ZGKF safemodes.

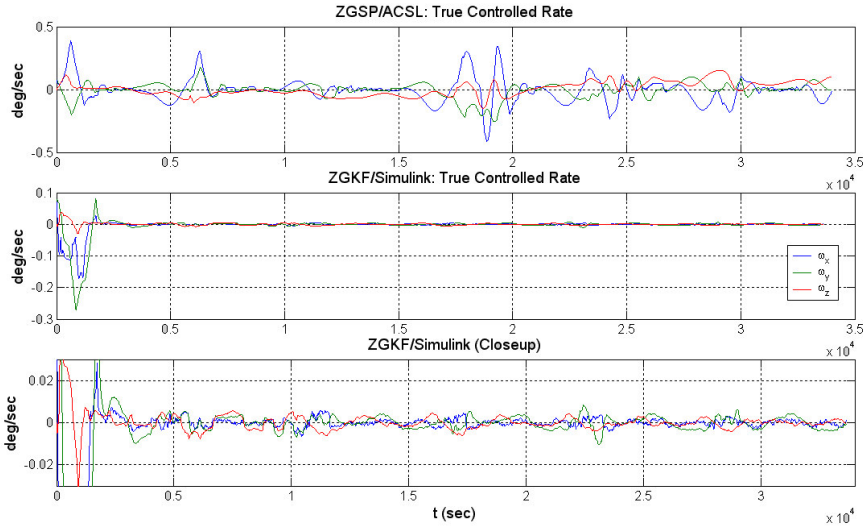

Figure 7. Comparison of rate history for ZGSP and ZGKF safemodes.

SUMMARY

The design of an attitude and rate estimator based on the Multiplicative Extended Kalman Filter was presented that can be used with the existing sun point controller with minor modification in gains to keep the Hubble Space Telescope in the sun pointing attitude when less than three gyros are available. This new safemode, called zero-gyro-Kalman-filter (ZGKF), utilizes the coarse sun sensor and magnetometer measurements to provide 3-axis rate and inertial quaternion estimates. Simulations show that the ZGKF performs better than the current zero-gyro sun point mode by keeping excursions during orbit night small by enabling control during this period. With ZGKF, the HST can be in a safemode with small position and rate errors making it a viable zero-gyro safemode for a rendezvous mission with the deorbit module.

REFERENCES

1. Markley, F. L., "Zero-Gyro Safemode Controller for the Hubble Space Telescope," *Journal of Guidance, Control, and Dynamics*, Vol. 17., No. 4, July-August 1994, p. 815-822.
2. Lee, S., et al, "Hubble Space Telescope Servicing Mission 3A Rendezvous Operations," University of Minnesota Control Science and Dynamical Systems Seminar, Sept. 26, 2003.
3. Gelb, A., *Applied Optimal Estimation*, The MIT Press, Cambridge, MA, 1974.
4. Markley, F. L., "Attitude Error Representations for Kalman Filtering," *Journal of Guidance, Control, and Dynamics*, Vol. 26, No. 2, March-April 2003, p. 311-317.
5. Wertz, J., *Spacecraft Attitude Determination and Control*, Kluwer Academic Publishers, Norwell, MA, 1978.